JOURNAL OF SOLID STATE CHEMISTRY 74, 356–368 (1988)

Structural Systematics around High T_c Superconductors $YBa_2Cu_3O_{6+x}$

JEAN GALY, RENÉE ENJALBERT, PATRICE MILLET,
CHRISTOPHE FAULMANN, AND PATRICK CASSOUX

*Laboratoire de Chimie de Coordination du CNRS, 205, route de Narbonne,
31077 Toulouse Cedex, France*

Received August 6, 1987; in revised form December 7, 1987

Starting from the ABO_3 perovskite structure a structural scheme is developed based on extended oxygen defects and on the yttrium/barium ordering. The $YBa_2Cu_3O_{9-n}$ series, with $n = 1, 2$, and 3, was derived from a "$YBa_2Cu_3O_9$" tri-perovskite through systematic rationalization of the oxygen loss. For each n value two possible polymorphs, (I) and (II), are selected. The structure of the $YBa_2Cu_3O_{6+x}$ series ($0 \leq x \leq 2$), containing the high T_c superconducting phases, results from A. D. Wadsley's ("Nonstoichiometric Compounds" (L. Mandlecorn, Ed.), Academic Press, New York (1964)) intergrowth defects combining these polymorphs. For $0 \leq x \leq 1$ such models imply the possibly simultaneous presence of Cu(I), Cu(II), and Cu(III) oxidation states; for $x \geq 1$ the presence of Cu(I) is no longer necessary. Following this structural scheme, theoretical powder patterns are calculated. They are in agreement with the experimental ones of $YBa_2Cu_3O_{6+x}$ phases prepared by standard procedures involving different annealing times. Conductivity measurements show that superconductivity above liquid nitrogen temperature is associated with a high oxygen content, i.e., $x > 0.66$. © 1988 Academic Press, Inc.

Introduction

The discovery of new high T_c superconducting ceramics derived from *Ln*–Ba–Cu oxide systems, explored by Michel and Raveau (*1*), seems to proceed, as usual, from well-planned accidents. Since the disclosure of superconductivity above 30 K in $La_{2-x}Ba_xCuO_4$ (*2*) and, more recently, above 90 K in $YBa_2Cu_3O_{6+x}$ (*3*), a very large number of papers from many different groups over the world have been published on this compound family (*4–14*).

Having been interested for a long time in nonstoichiometry phenomena in mixed-valence vanadium oxibronzes, excess fluorite MO_{2+x} family compounds, extended Wadsley's defects in hexagonally close-packed structures or perovskites series ABO_{3+x} (Galy *et al.* (*15*)), and new molecular superconductors (Cassoux *et al.* (*16*)), it was tempting to follow the rush on these new high T_c superconducting nonstoichiometric ternary oxides and to try to apply our own experience on the subject.

Although the oxygen content in these ceramics clearly is a key factor in determining their superconducting properties, a systematic rationalization of this factor has not yet been established, nor discussed in detail.

We report in this paper the synthesis, characterization, and resistivity study of $YBa_2Cu_3O_{6+x}$ phases, based on a structural scheme which helps in understanding the

0022-4596/88 $3.00

possible mechanisms of nonstoichiometry associated with the gain or the loss in oxygen.

Structural Scheme

(*I*) *The* $YBa_2Cu_3O_{9-n}$ *Series* (*with* $0 \leq n \leq 3$)

Our aim in this section is to systematize the possibilities of oxygen nonstoichiometry in the basic perovskite formula of the new superconducting ceramics, in order to obtain a useful structural picture of their remarkable composition versatility and to follow their chemical compositions.

The perovskite structure ABO_3 is a well-known cubic structure ($BaTiO_3$, for example) in which the oxygen and A atoms form a cubic close-packed array (Fig. 1). The B atoms occupy the octahedral sites and the A atoms the center of oxygen cuboctahedra, CN = 12. The octahedra share their vertices and the cuboctahedra their square faces in the three crystallographic directions.

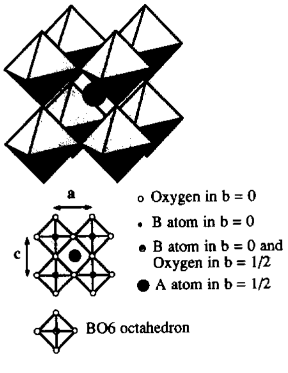

FIG. 1. The ABO_3 perovskite structure and its representation.

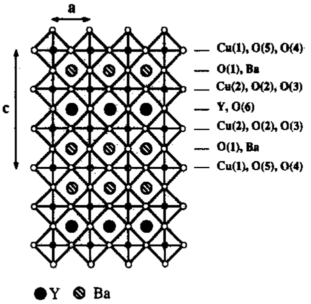

FIG. 2. The "$YBa_2Cu_3O_9$" ordered structure, or "tri-perovskite," created by a 1-2 order between one yttrium and two barium layers.

In order to discuss the mechanisms of nonstoichiometry in such a structure, it is necessary to imagine a hypothetical stoichiometric perovskite "$YBa_2Cu_3O_9$." It could be objected that, chemically, the $YBa_2Cu_3O_9$ form seems to be impossible to obtain, for it implies the presence of Cu(IV), i.e., $YBa_2Cu^{III}Cu_2^{IV}O_9$. It should be noted however that this hypothetical form may be formally obtained through F to O substitutions involving Cu(II), Cu(I), Cu(III), or mixtures of them. Nevertheless, the point we would like to emphasize here is the ordering of yttrium and barium atoms in planes, which determines a structural order having the tripling of the c axis as a consequence. Such a structure (Fig. 2) should crystallize in a tetragonal system, space group *P4/mmm*. However, it has been shown that small orthorhombic distortion can occur in $YBa_2Cu_3O_7$ and, therefore, the space group *Pmmm* derived by Siegrist *et al.* (*8*) can be conveniently used to describe this phase and the whole $YBa_2Cu_3O_{9-n}$ series (see Table I). By analogy with the trirutile or tri-αPbO_2 (*17*), AB_2O_6 structures that show similar cation ordering, this basic structure is named the tri-perovskite $YBa_2Cu_3O_9$.

$YBa_2Cu_3O_8$. On the basis of this tri-perovskite structure it is then possible to play with oxygen extended defects (Wadsley's intergrowth defects (*18–19*)), to go down to the lower stoichiometry, $YBa_2Cu_3O_8$, in which all the copper atoms should be in the oxidation state (III), i.e., formally $YBa_2Cu_3^{III}O_8$. Two possibilities

TABLE I

LIST OF ATOMS, SITES, COORDINATES, AND OCCUPANCY FACTORS FOR THE $YBa_2Cu_3O_{9-n}$ AND $YBa_2Cu_3O_{6+x}$ SERIES

Atom	Site	Coordinates			$YBa_2Cu_3O_{9-n}$				$YBa_2Cu_3O_{6+x}$
					$n = 0$	1	2	3	$0 \leq x \leq 1$
Ba	2t	$\frac{1}{2}$	$\frac{1}{2}$	0.166	1	1	1	1	1
Y	1h	$\frac{1}{2}$	$\frac{1}{2}$	$\frac{1}{2}$	1	1	1	1	1
Cu(1)	1a	0	0	0	1	1	1	1	1
Cu(2)	2q	0	0	0.333	1	1	1	1	1
O(1)	2q	0	0	0.166	1	1	1	1	1
O(2)	2s	$\frac{1}{2}$	0	0.333	1	1	1	1	1
O(3)	2r	0	$\frac{1}{2}$	0.333	1	1	1	1	1
O(4)	1e	0	$\frac{1}{2}$	0	1	1	1	0	x
O(5)	1b	$\frac{1}{2}$	0	0	1	1	0	0	0
O(6)	1c	0	0	$\frac{1}{2}$	1	0	0	0	0

Occupancy factors: 1 ⇒ 100%, 0 ⇒ 0%, and $x \Rightarrow x\%$

Note. The space group used is *Pmmm*.

have been retained resulting in two reasonable structures:

—The first structure, $YBa_2Cu_3O_8$(I), is formed by pulling out strings of oxygen atoms located on the $\{x, \frac{1}{2}, 0\}$ line (Fig. 3a); the vacancies so created transform CuO_6

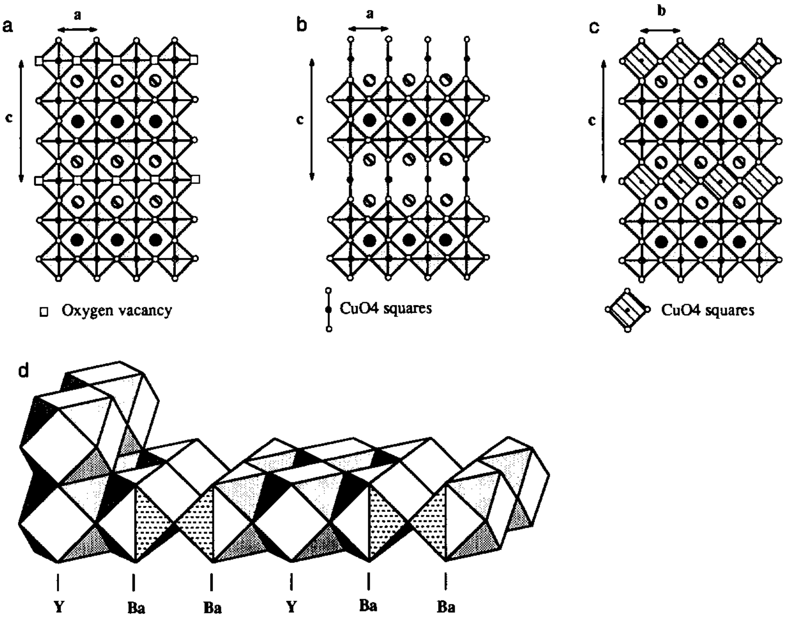

FIG. 3. The $YBa_2Cu_3O_8$(I) structure: (a) Oxygen vacancies in the tri-perovskite; (b) projection onto the (010) plane; (c) projection onto the (100) plane; (d) the sequence of YO_{12} cuboctahedra and Ba_2O_{18} polyhedra along the c axis.

octahedra (*O*) into CuO_4 squares (*S*). This three-dimensional structure exhibits then a double layer of CuO_6–*O* connected to each other in the [001] direction by corner sharing with a continuous chain of CuO_4–*S* (Figs. 3b and 3c). The structure should exhibit an orthorhombic distortion, with $a < b$, due to . . . -O-Cu-O-Cu-O- . . . bonding along the *b* axis (diagonal of the CuO_4–*S*), the space group becoming *Pmmm*. The yttrium atoms are still in cuboctahedra but the barium atoms are in polyhedra having 10 vertices (CN = 10) and built up by a square antiprism (half cuboctahedron) sharing its large square with a trigonal prism. Two of these BaO_{10} polyhedra are held together via edge sharing along [010] making Ba_2O_{18} units. The network of the YO_{12} cuboctahedra and Ba_2O_{18} polyhedra is shown in Fig. 3d.

—The second structure, $YBa_2Cu_3O_8$(II), can be obtained by removing the oxygen layer in (001) plane at the level of Y atoms (Fig. 4a), giving rise to a structure consisting of one layer of CuO_6–*O* in between two layers of CuO_5 square pyramids (*SP*); all of these polyhedra share corners (Fig. 4b). The structure should crystallize in the tetragonal system, i.e., *P*4/*mmm*. The barium atoms are still in double slabs of cuboctahedra, but the yttrium atoms are located in a plane bordered by the bases of the CuO_5–*SP*, i.e., in square prisms (CN = 8). The sequence of two BaO_{12} cuboctahedra connected by face sharing with YO_8 square prisms along [001] is schematized in

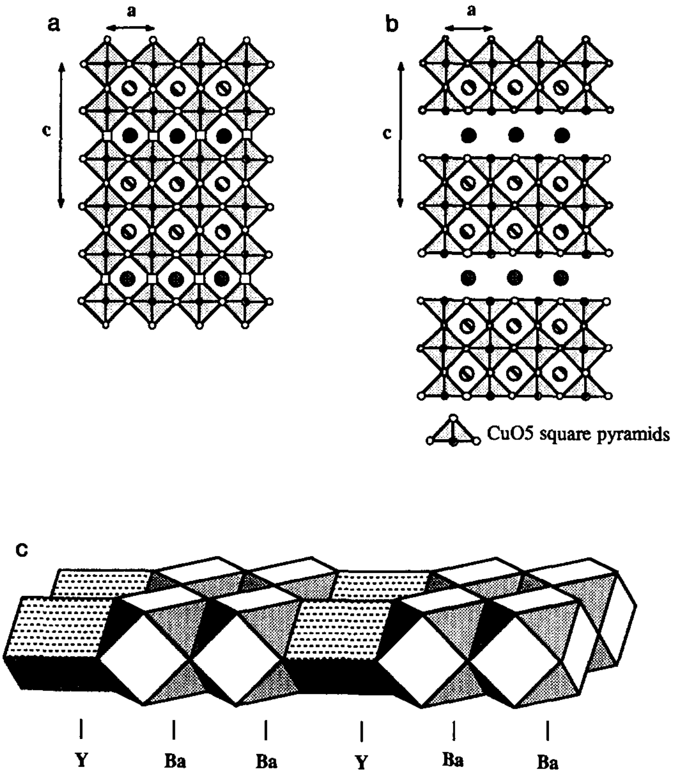

FIG. 4. The $YBa_2Cu_3O_8$(II) structure: (a) Oxygen vacancies in the tri-perovskite; (b) projection onto the (010) plane (the same onto the (100) plane); (c) the sequence of YO_8 square prisms and BaO_{12} cuboctahedra along the *c* axis.

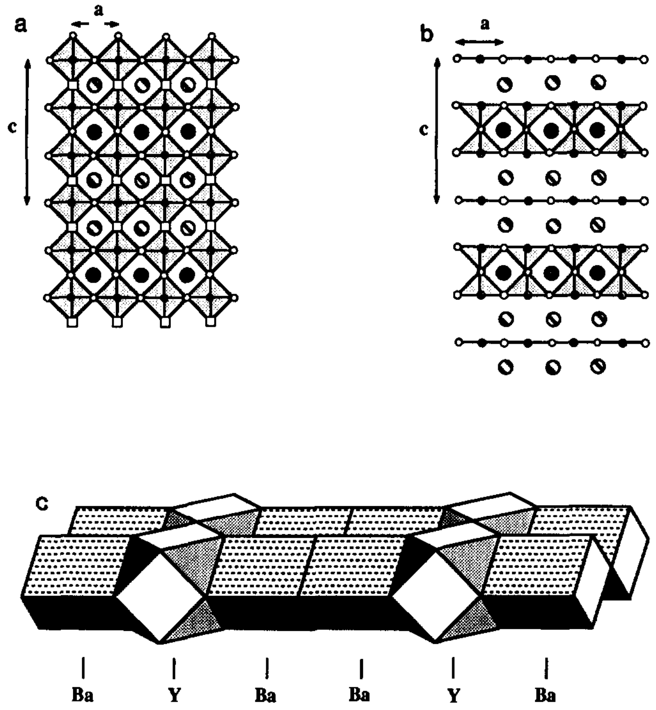

FIG. 5. The $YBa_2Cu_3O_7$(I) structure: (a) Oxygen vacancies in the tri-perovskite; (b) projection onto the (010) plane (the same onto the (100) plane); (c) the sequence of YO_{12} cuboctahedra and two BaO_8 square prisms along the *c* axis.

Fig. 4c. It is interesting to note that the same form II has been previously proposed by Michel *et al.* (*7*).

$YBa_2Cu_3O_7$. This structure corresponds to the stoichiometric superconducting phase. It is a mixed valence compound, i.e., $YBa_2Cu_2^{II}Cu^{III}O_7$. This stoichiometry can be achieved by pulling out two strings of oxygen in the basic tri-perovskite structure. Again two reasonable possibilities can be envisioned:

—$YBa_2Cu_3O_7$(I), after oxygen removal (Fig. 5a), exhibits a double layer of CuO_5–*SP*, imbedding yttrium atoms in cuboctahedra and a layer of CuO_4–*S* parallel to the (001) plane in between the layers of barium atoms (Fig. 5b); such a network should be tetragonal. The barium atoms are located in square prisms sharing square faces along [001] and edges in the [100] and [010] direction (see Fig. 5c).

—$YBa_2Cu_3O_7$(II), the idealized structure of Capponi *et al.* (*10*), is directly derived from the tri-perovskite by pulling out two strings of oxygen atoms from the {$\frac{1}{2}$, *y*, 0} and {*x*, 0, $\frac{1}{2}$} rows (Fig. 6a).

Alternatively, the $YBa_2Cu_3O_7$(II) form can be derived from $YBa_2Cu_3O_8$(II) by pulling out the string of oxygen atoms of the octahedra layer (see Fig. 4b). In this structure a triple slab is formed by two layers of CuO_5–*SP* held together by a layer of corner sharing CuO_4–*S* (Figs. 6b and 6c). Capponi *et al.*'s (*10*) criticism of Siegrist *et al.*'s (*8*) paper appears founded: a disorder on the sites O(4) and O(5), occupied at 50%, should reasonably give rise to a tetragonal structure instead of the demonstrated

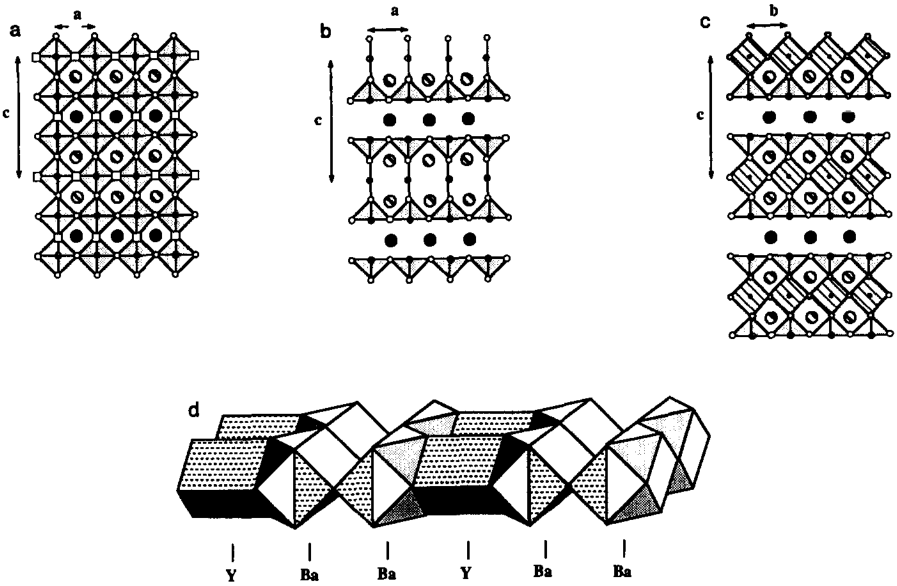

FIG. 6. The $YBa_2Cu_3O_7$(II) structure: (a) Oxygen vacancies in the tri-perovskite; (b) projection onto the (010) plane; (c) projection onto the (100) plane; (d) the sequence of YO_8 square prisms and Ba_2O_{18} polyhedra along the *c* axis.

orthorhombic one. In this structure, yttrium atoms are in square prisms (CN = 8) sharing edges in the [010] direction and the barium atoms are in the Ba_2O_{18} polyhedra already described for $YBa_2Cu_3O_8$(I). The YO_8 square prisms share edges in the [100] direction while the Ba_2O_{18} polyhedra share their trigonal faces along [100] and their square faces along [010] (Fig. 6d).

Both I and II forms correspond to the copper oxidation states of the formula, with a ratio of CuO_5–*SP* (Cu^{II}) over CuO_4–*S* (Cu^{III}) equal to 2. The structural studies of $YBa_2Cu_3O_7$ compounds performed by X-ray single crystal (Siegrist *et al.* (*8*), Calestani and Rizzoli (*9*)) and neutron powder diffraction (Capponi *et al.* (*10*); Beech *et al.* (*11*)) lead to a structure which is similar to form II described above. Therefore, form II is to be preferred according to these experimental results.

$YBa_2Cu_3O_6$. This stoichiometric formula implies the simultaneous presence of copper (I) and (II), i.e., $YBa_2Cu^{II}_2Cu^{I}O_6$. One simple way to remove oxygen of the structure is to empty all the oxygen rows located in the plane of the yttrium and barium atoms and perpendicular to the *c* axis (Fig. 7a). The resulting tetragonal structure $YBa_2Cu_3O_6$(I) consists of a layered structure of corner sharing CuO_4–*S*, of composition $(CuO_2)_n$, interleaved with the planar sequence . . . Ba . . . Ba . . . Y . . . Ba . . . Ba . . . Y . . . (Fig. 7b). All the barium and yttrium atoms are in square prisms sharing edges along [100] and [010] and faces along [001] (Fig. 7c). In fact, this solution implies a square coordination for Cu^{I}, yet unknown, the favored ones being the linear O–Cu–O, the planar CuO_3, the pseudo-tetrahedral CuO_{3+1}, and the tetrahedral CuO_4.

The second model, also tetragonal, $YBa_2Cu_3O_6$(II), is derived from the tri-perovskite by pulling out the oxygen rows in the yttrium plane and all the oxygens in the (100) planes (Fig. 8a) and exhibits the following remarkable feature: it consists of a triple layer built up with two layers of square pyramids held together via their apices, by a copper atom in a linear twofold coordination (*L*), CuO_2–*L* (Fig. 8b). The chemical formula is then perfectly acquainted with a ratio of CuO_5–*SP*/CuO_2–*L* equal to 2.

The structural studies of $YBa_2Cu_3O_6$ compounds by neutron powder diffraction (Santoro *et al.* (*12*)) and X-ray single crystal (Swinnea and Steinfink (*13*)) coincides with form II described above. Therefore, $YBa_2Cu_3O_6$ form II should be preferred at this point.

In this structural model, the barium atoms are in pseudo-square antiprisms (CN = 8; half cuboctahedra) sharing edges and corners along [100] direction, trigonal faces along [010], and nothing along the *c* axis (Fig. 8c). The yttrium atoms are sitting in square prisms bidimensionally associated via edges along *a* and *b* axes and sharing their square faces with the BaO_8 square prisms along [001]. The rigidity of the network is ensured by copper (I) in its linear coordination, holding together the BaO_8 polyhedra. Two consecutive BaO_8 polyhedra along [001] have no oxygen in common, and so a small displacement of Ba atoms is expected; they move toward the center of their polyhedra, the consequence being an increased value of the Ba–Ba distance along the *c* axis.

This whole discussion, using extended defects to describe the possible structures, step by step, from the stoichiometry $YBa_2Cu_3O_9$ down to $YBa_2Cu_3O_6$ allows one now to propose a plausible structural construction for the compound $YBa_2Cu_3O_{6.5}$. This composition may be obtained from an ap-

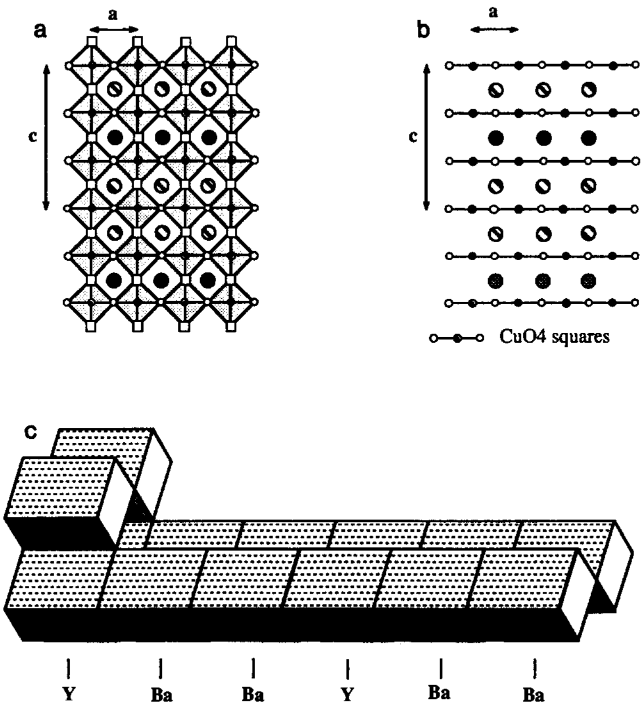

FIG. 7. The $YBa_2Cu_3O_6$(I) structure: (a) Oxygen vacancies in the tri-perovskite; (b) projection onto the (010) plane (the same onto the (100) plane); (c) the sequence of YO_8 and BaO_8 square prisms along the *c* axis.

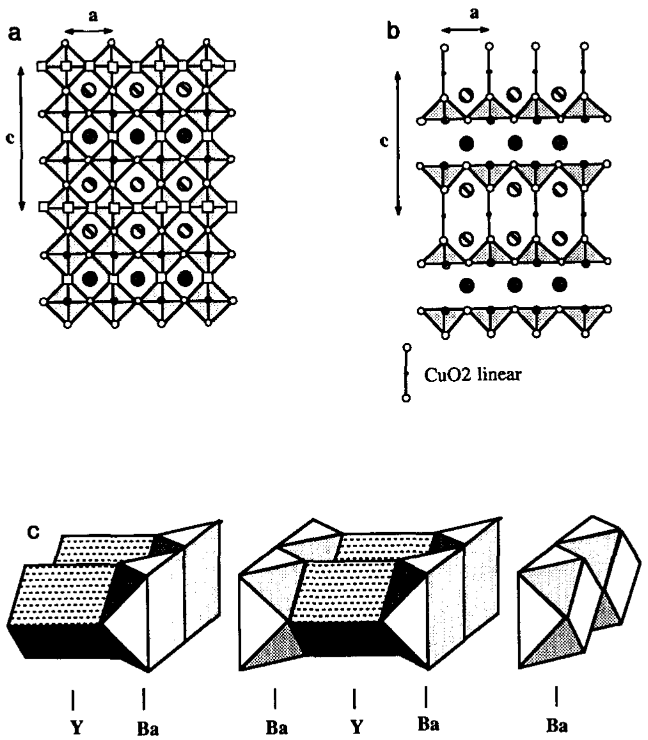

FIG. 8. The $YBa_2Cu_3O_6$(II) structure: (a) Oxygen vacancies in the tri-perovskite; (b) projection onto the (010) plane (the same onto the (100) plane); (c) the sequence of YO_8 square prisms and BaO_8 square antiprisms along the *c* axis.

propriate mixture Y_2O_3–4BaO–6CuO and should contain only divalent copper. However, a disproportionation process, 2Cu(II) → Cu(I) + Cu(III), is already possible at this stage. When the compound is exposed to oxygen at high temperature, oxidation of Cu(II) (and possibly Cu(I)) to Cu(III) occurs. It is also important to note that using $BaCO_3$ instead of BaO in the starting mixture may induce a partial oxidation of some Cu(II) to Cu(III) prior to any exposition to oxygen.

(II) The $YBa_2Cu_3O_{6+x}$ Series ($0 \leq x \leq 2$)

$0 \leq x \leq 0.5$ . . . *up to* $YBa_2Cu_3^{II}O_{6.5}$. One of the proposed structural schemes for this limit composition is illustrated in Fig. 9; it consists of a simple intergrowth $YBa_2Cu_3O_7$(II)/$YBa_2Cu_3O_6$(II).

Formally, for the whole series the copper charge is in between (I) and (II) and the structures can be described by simple intergrowths, as already demonstrated for complicated ABO_{3+x} oxygen-excess perovskite phases by Galy *et al.* (*15*). Then, all the compositions corresponding to very small variations of *x* can be depicted by these intergrowths, ordered, disordered, or exhibiting complicated orders (cells of up to 1300 Å in one crystallographic direction corresponding to ordered intergrowths have been found in ABO_{3+x}). For different values of *x* the structure can be described by introducing, in the structure of $YBa_2Cu_3O_{6.5}$, more $\{Cu_3O_6\}$ slabs of the type already shown in Fig. 8b.

$0.5 \leq x \leq 1$ . . . *up to* $YBa_2Cu_2^{II}Cu^{III}O_7$. A reference compound $YBa_2Cu_3O_{6.666}$ is

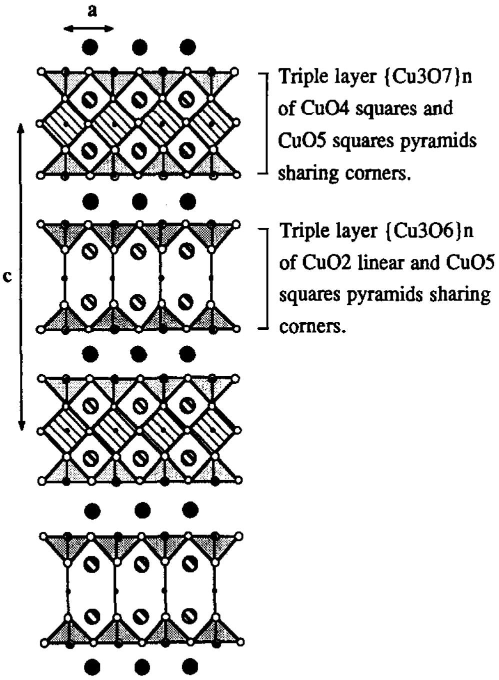

FIG. 9. Projection of the $YBa_2Cu_3O_{6.5}$ structure onto the (010) plane. The structure is the result of a perfect intergrowth of the $YBa_2Cu_3O_7$(II) and the $YBa_2Cu_3O_6$(II) networks.

shown in Fig. 10. It is easy to imagine the structure for other compositions. The stoichiometry in this region of composition will be very difficult, and probably even impossible, to ascertain. It will depend on the temperature, time of treatment, oxygen pressure, quenching rate, etc., and several phases can be present in the different parts of the crucible. Nevertheless, and fortunately, in well-controlled synthesis, one of these phases must be present in majority, with a narrow dispersion of the histogram composition of the crystallites around it; this sort of situation has been enlightened by Andersson and Leygraf (*20*) in their study of the nonstoichiometry of the defect Ru_4Si_3 alloy.

$1 \leq x \leq 2$ . . . up to $YBa_2Cu_3^{III}O_8$. The same structural principles can be applied, the intergrowth being achieved, starting from $YBa_2Cu_3O_7$(II), for example, and introducing $\{Cu_3O_8\}_n$ slabs. The structure of $YBa_2Cu_3O_{7.333}$ corresponding to two slabs of $\{Cu_3O_7\}_n$ for one of $\{Cu_3O_8\}_n$ is given as an example in Fig. 11.

Conclusion

This systematic structural discussion reveals the importance of the Y/Ba order and of the ability of the Y, Ba, and Cu atoms to accommodate various coordination polyhedra ($8 \leq CN \leq 12$ for Y and Ba, shown in Fig. 12, and $2 \leq CN \leq 6$ for Cu). Such a flexibility in the coordination of the Y and Ba atoms allows compensation for the

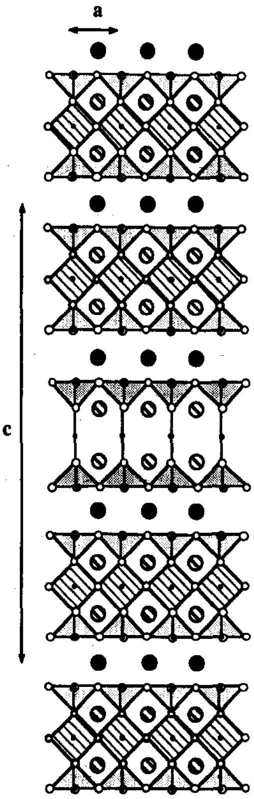

FIG. 10. Projection of the $YBa_2Cu_3O_{6.666}$ structure onto the (010) plane. The structure is the result of a perfect intergrowth of two $YBa_2Cu_3O_7$(II) and one $YBa_2Cu_3O_6$(II) networks.

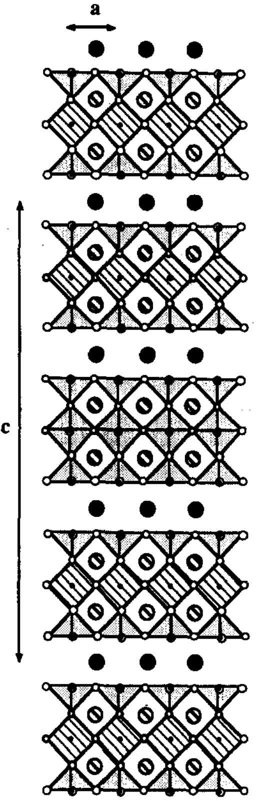

FIG. 11. Projection of the $YBa_2Cu_3O_{7.333}$ structure onto the (010) plane. The structure is the result of a perfect intergrowth of two $YBa_2Cu_3O_7$(II) and one $YBa_2Cu_3O_8$(II) networks.

changes in the coordination of the Cu atom in its different oxydation states (I), (II), and (III).

Such models evidence the possibility of having both Cu^{I} and Cu^{III} coexisting in the structure together with Cu^{II}. It should also be noted that, in the retained model for $YBa_2Cu_3O_{6.5}$ with $0 \leq x \leq 1$ built on the forms II of the limit compounds, the Y atoms keep their intact polyhedra, i.e., YO_8 square prisms. The "oxygen adjustment" is achieved in between the Ba layers and results in the transformation of two consecutive BaO_8 square antiprisms in Ba_2O_{18} polyhedra units; this is supported by an EXAFS study on the Y-adsorption edge at Lure (Orsay, France) by Dartyge *et al.* (*21*).

We will now show, in a short and preliminary example, that this structural approach may be used as a guideline to rationalize the chemistry and the characterization investigations with a systematic spirit.

Synthesis and Characterization of the $YBa_2Cu_3O_{6+x}$ Series

The synthesis of the $YBa_2Cu_3O_{6+x}$ phases followed standard procedures. This involved intimate mixing of the corresponding oxide and carbonate powders in the molar ratio $Y_2O_3/4BaCO_3/6CuO$. This mixture was finely ground in an agate mortar and pestle and heated in a mullite boat in air at 950°C for 12 hr. The resulting powder was ground again and pressed into pellets ($10\ T \cdot cm^{-2}$) of 10 mm diameter and 1 mm thickness. These pellets were annealed at 950°C under oxygen flow for different periods from 4 up to 8 hr. The rate of cooling of the oven was kept as slow as $2°C \cdot min^{-1}$.

In order to check the relevance of our structural scheme, especially to verify whether, with Y, Ba, and Cu as heavy ions, the variable presence of oxygen on preferential sites is detectable, theoretical powder patterns were calculated for increasing values of x in the $YBa_2Cu_3O_{6+x}$ formula, by varying the occupation ratio of the O(4) site at $0\ \frac{1}{2}\ 0$. These calculations were performed by using the Lazy-Pulverix software (*22*).

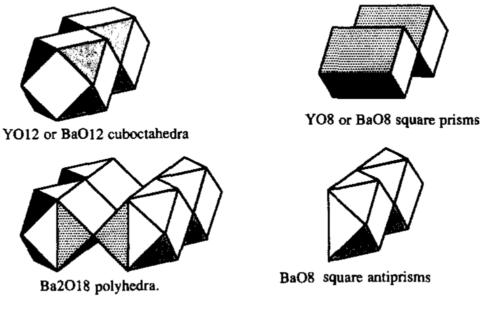

YO12 or BaO12 cuboctahedra

YO8 or BaO8 square prisms

Ba2O18 polyhedra.

BaO8 square antiprisms

FIG. 12. Various polyhedra in $YBa_2Cu_3O_{6+x}$ phases.

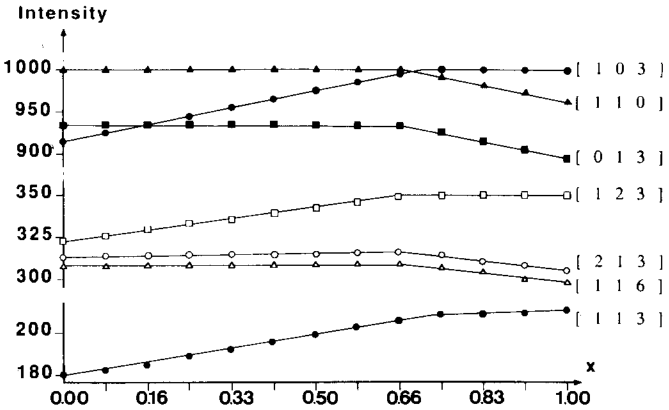

FIG. 13. Variations of the theoretical intensity of some X-ray powder pattern lines in the $YBa_2Cu_3O_{6+x}$ series as a function of the occupation ratio of the O(4) sites at 0 ½ 0 ($0 \leq x \leq 1$).

They were based on the atomic coordinates and cell parameters obtained at 300 K by Capponi *et al.* (*10*) from a neutron powder structural study (a = 3.8206, b = 3.8851, c = 11.6757 Å). The variations of the theoretical intensity of selected lines are presented in Fig. 13; for all the lines, slope change is clearly observed at ca. x = 0.66. It is interesting to note that this x = 0.66 composition corresponds, for the first time in the series, to the association in pairs of all Cu(II)–Cu(III) containing $(Cu_3O_7)_n$ slabs. As will be shown later, this fact seems to be associated with the occurrence of superconductivity above liquid nitrogen temperature in such phases.

Systematic X-ray powder patterns were collected before and after annealing under oxygen flow. The oxygen content was approximately determined by weighting these samples before and after annealing. Figure 14 shows the powder pattern (32° ≤ 2θ ≤ 33°) of three selected $YBa_2Cu_3O_{6+x}$ samples with $x \approx$ 0.5, 0.66, and 0.75, which corresponds to 0-, 4-, and 8-hr annealing times, respectively. The relative intensity of the (013) peak, with respect to the intensity of the peak resulting from the (103) and (110) reflections, decreases when x increases, i.e., when the annealing time is increased. These relative intensity variations are consistent with those, theoretically calculated for the same reflections, shown in Fig. 13. However, this comparison between experimental and theoretical intensities remains qualitative, because it is impossible to estimate the respective contributions of the

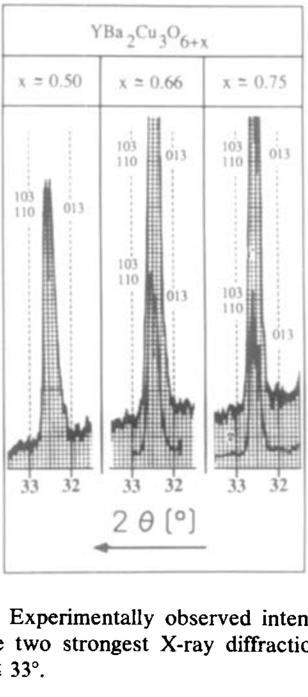

FIG. 14. Experimentally observed intensity variation of the two strongest X-ray diffraction lines at 32° ≤ 2θ ≤ 33°.

(103) and (110) reflections which are separated for Cu*Kα* radiation by only $\Delta\theta = 0.04°$.

Electrical contacts to small chips ($8 \times 3 \times 2$ mm^3) cut out of the pellets were made by using Emetron M8001 gold paint. The resistance of the contacts was typically 1 Ω. Four-probe conductivity measurements were carried out by using an RV Elektroniika Oy, Model AVS 45-L automatic resistance bridge. The room temperature resistance of the superconducting samples was typically 0.03 Ω. The mounted samples were placed in an Oxford Instruments CF200 continuous flow cryotstat for temperature-dependent measurements. Monitoring of the temperature variations (as slow as 0.1 K $\cdot$ min^{-1}) and data acquisition were achieved using an Oxford Instruments DTC2 temperature controller driven by an Apple IIe microcomputer equipped with specific home-made interfaces (*23*) (analogic monitoring of the DTC2; analogic temperature acquisition; parallel input–output resistance acquisition). The lowest resistance that can be measured with this apparatus is 10^{-5} Ω. The superconducting state of the sample, i.e., the expulsion of a magnetic field, has been checked by observation of the hovering of a small magnet above the sample cooled by liquid nitrogen.

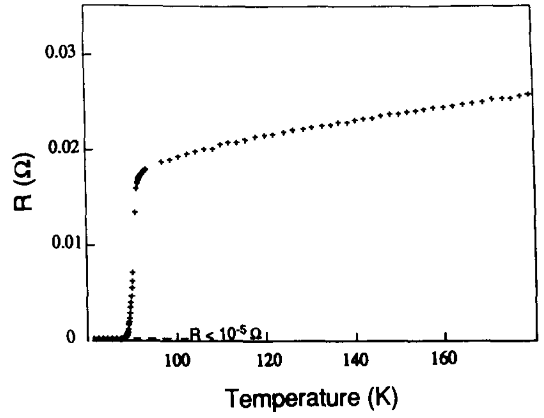

FIG. 15. Plot of four-probe electrical resistivity vs temperature for $YBa_2Cu_3O_{6.75}$.

As previously observed (*5*), when the samples were not annealed under oxygen flow, or annealed only in air, no superconducting transition was observed above liquid nitrogen temperature. Annealing under oxygen flow for periods longer than 4 hr raised T_c above this temperature. The highest T_c and sharpest transitions were obtained for an annealing time reaching 8 hr, i.e., for an $x \geq 0.75$ oxygen content. Figure 15 shows the resistivity vs temperature curve of the $YBa_2Cu_3O_{6.75}$ sample (annealing time 8 hr). The onset temperature of the superconducting transition is 93 K. Below 88 K the resistance is smaller than 10^{-5} Ω.

References

1. C. MICHEL AND B. RAVEAU, *Rev. Chim. Miner.* **21,** 407 (1984).
2. J. G. BEDNORZ AND K. A. MULLER, *Z. Phys. B* **64,** 189 (1986).
3. M. K. WU, J. R. ASHBURN, C. J. TORNG, P. H. HOR, R. L. MENG, L. GAO, Z. J. HUANG, Y. Z. WANG, AND C. W. CHU, *Phys. Rev. Lett.* **58,** 908 (1987).
4. R. J. CAVA, B. BATLOGG, R. B. VAN DOVER, D. W. MURPHY, S. SUNSHINE, T. SIEGRIST, J. P. REMEIKA, E. A. RIETMAN, S. ZAHURAK, AND G. ESPINOSA, *Phys. Rev. Lett.* **58,** 1676 (1987).
5. E. M. ENGLER, V. Y. LEE, A. I. NAZZAL, R. B. BEYERS, G. LIM, P. M. GRANT, S. S. P. PARKIN, M. L. RAMIREZ, J. E. VAZQUEZ, AND R. J. SAVOY, *J. Amer. Chem. Soc.* **109,** 2848 (1987).
6. C. N. R. RAO, P. GANGULY, A. K. RAYCHAUDHURI, R. A. MOHAN RAM, AND K. SREEDHAR, *Nature* (*London*) **326,** 856 (1987).
7. C. MICHEL, F. DESLANDES, J. PROVOST, P. LEJAY, R. TOURNIER, M. HERVIEU, AND B. RAVEAU, *C.R. Acad. Sci. Paris, Ser. II* **304,** 1059 (1987).
8. T. SIEGRIST, S. SUNSHINE, D. W. MURPHY, R. J. CAVA, AND S. M. ZAHURAK, *Phys. Rev. B* **35,** 7137 (1987).
9. G. CALESTANI AND C. RIZZOLI, *Nature* (*London*) **328,** 606 (1987).
10. J. J. CAPPONI, C. CHAILLOUT, A. W. HEWAT, P. LEJAY, M. MAREZIO, N. NGUYEN, B. RAVEAU, J. L. SOUBEYROUX, J. L. THOLENCE, AND R. TOURNIER, *Europhys. Lett.* **3,** 301 (1987).
11. F. BEECH, S. MIRAGLIA, A. SANTORO, AND R. S. ROTH, *Phys. Rev. B* **35,** 8778 (1987).

12. A. Santoro, S. Miraglia, F. Beech, S. A. Sunshine, D. W. Murphy, L. F. Schneemeyer, and J. V. Waszczak, *Mater. Res. Bull.* **22,** 1007 (1987).
13. J. S. Swinnea and H. Steinfink, *J. Mater. Res.* **2,** 424 (1987).
14. H. Ihara, M. Hirabayashi, N. Terada, Y. Kimura, K. Senzaki, M. Akimoto, K. Bushida, F. Kawashima, and R. Uzuka, *Japan. J. Appl. Phys.* **26,** L460 (1987).
15. J. Galy, *Bull. Soc. Fr. Miner. Cristallogr.* **94,** 250 (1971); S. Andersson and J. Galy, *J. Solid State Chem.* **1,** 339 (1970); J. Galy and R. S. Roth, *J. Solid State Chem.* **7,** 277 (1973); R. Portier, A. Carpy, J. Galy, and M. Fayard, *Phys. Status Solidi* **30,** 683 (1975).
16. L. Brossard and M. Ribault, M. Bousseau, L. Valade, and P. Cassoux, *C.R. Acad. Sci. Paris, Ser. II* **302,** 205 (1986); L. Brossard, M. Ribault, L. Valade, and P. Cassoux, *Physica B* **143,** 378 (1986); J. E. Schirber, D. L. Overmyer, J. M. Williams, H. H. Wang, L. Valade, and P. Cassoux, *Phys. Lett.* **120,** 87 (1987).
17. J. Galy and J. Senegas, *C.R. Acad. Sci. Paris, Ser. II* **275,** 665 (1972).
18. A. D. Wadsley, "Nonstoichiometric Compounds" (L. Mandelcorn, Ed.), Academic Press, New York (1964).
19. S. Andersson and A. D. Wadsley, *Nature (London)* **211,** 581 (1966).
20. S. Andersson and C. Leygraf, *J. Solid State Chem.* **14,** 78 (1975).
21. E. Dartyge, personal communication.
22. K. Yvon, W. Jeitschko, and E. Parthe, *J. Appl. Crystallogr.* **10,** 73 (1977).
23. R. Dartiguepeyron, unpublished results.